IJBBE International Journal of Biophotonics & Biomedical Engineering Vol. 3, No. 1, Winter-Spring, 2023

Research Article

Effect of Protein Corona Formation on Photonic Response of Upconverting Nanoparticles

N. Ghazyani[a], M. MajlesAra* [a,b]

a Faculty of Physics, Kharazmi University, Tehran, Iran
b Applied Science Research Center, Kharazmi University, Tehran, Iran

*** Corresponding Author Email: majlesara@gmail.com**

DOI: 10.30495/ijbbe.2023.1985468.1025

ABSTRACT

Received: May. 6, 2023, Revised: Jul. 9, 2023, Accepted: Sep. 17, 2023, Available Online: Sep. 22, 2023

NaYF4:Yb, Er is one of the efficient and well-known upconverting materials which emit photoluminescence light at 545 nm and 660 nm under an excitation of 980 nm. In this study, up-conversion nanoparticles using the thermal decomposition method have been synthesized and characterized, and phase transition from organic to aquas by synthesis of a SiO2 shell has been done successfully. The results show that the nonlinearity response of NaYF4: Yb, Er@SiO2 is the same as NaYF4: Yb, Er, and SiO2 does not affect emission peaks. It means that these nanoparticles are suitable for biomedical applications. Since it is necessary to know the photoluminescent behavior of UCNPs@SiO2 particles, thereby the fluorescence properties of up-conversion nanoparticles with SiO2 shell have been investigated in PBS, normal, and cancerous human blood plasma. The results indicate that UCNP@SiO2 can be applicable in biological media for therapy and diagnosis.

KEYWORDS

Nonlinear Photoresponse, Up-conversion Nanoparticles, Protein Corona, Corona Formation, Human Blood Plasma, Near-infrared.

I. INTRODUCTION

Up-conversion nanoparticles (UCNPs) are an emerging type of luminescent nanomaterials that can convert low-energy photons into high-energy ones through nonlinear optical processes [1], which makes them ideal for a wide range of applications, including bioimaging [2], therapy [3], detection [4], sensing [5], energy [6] and catalysis [7]. The Up-conversion photoluminescence phenomenon occurs when there are electronic transitions between 4f orbitals within a single lanthanide ion. These transitions have wave functions that are localized within the ion. The 4f electrons are shielded by the outer 5s and 5p shells, resulting in sharp emissions resembling lines. Typically, the intra-4f electronic transitions of lanthanide ions are forbidden electric dipoles according to quantum mechanical selection rules. However, these rules can be relaxed due to the local crystal field-induced intermixing of the f states with

higher electronic configurations. The primary reason for the forbidden nature of the 4f–4f transition is its long lifetime. Energy levels of lanthanide ions have very long lifetimes, often lasting up to tens of milliseconds. This extended lifetime promotes sequential excitations to occur. [8]. An up-conversion system contains ions of absorber and activator that can emit visible or ultraviolet photons by energy transfer mechanisms. The dopants, such as Yb and Nd ions can efficiently absorb near-infrared (NIR) light and ions activator such as Er, Tm, Ho, etc. However, the biological applications of UCNPs are limited by their stability and compatibility in physiological environments, such as biological fluids or tissues [9]. To overcome the limitations of UCNPs, researchers have developed various surface modifications that can improve their stability and biocompatibility [10].

Usually in thermal decomposition for the synthesis of UCNPs organic solvents and surfactants are used, which can strongly bind to the surface of UCNPs and stabilize them in the organic solvents. For transferring the particles to water, the hydrophobic surface coating needs to be replaced with a hydrophilic surface coating, which can be accomplished by ligand exchange or coating [11]. The coating is one of the best methods of surface modification, which involves the deposition of a thin layer of a hydrophilic material such as silica, polymers, and PEG on the surface of the UCNPs [12]. This can be done by chemical deposition, electrostatic coating, or physical adsorption methods. One promising approach is to encapsulate UCNPs with dense silica shells ($dSiO_2$), which can prevent their degradation and enhance their dispersibility while minimizing their toxicity [13].

SiO_2 is a good material that is safe for use in living organisms and can be used to form a protective coating around nanoparticles. This coating can prevent the nanoparticles from breaking down or sticking together, and can also be used to deliver drugs to specific parts of the body. The SiO_2 coating can be formed using a chemical process such as sol-gel, which involves the use of a silicon alkoxide precursor such as tetraethyl orthosilicate (TEOS) [14], [15]. SiO_2 coatings not only can improve the biocompatibility of the nanoparticles but also reduce the side effects. This makes SiO_2-coated nanoparticles useful for biomedical applications such as imaging and drug delivery. Consequently, the use of SiO_2 coatings for nanoparticles provides several benefits, including improved solubility, stability, and biocompatibility, making them a promising material for a range of applications. However, for using UCNPs shelled by SiO_2, there are still gaps in understanding how SiO_2 shells affect the properties of UCNPs when used in a biological medium [16]. Therefore, in this study, two important points are investigated. The first one: up-converted fluorescence of UCNP@SiO_2 in water and phosphate-buffered saline (PBS). The second one: how the formation of protein corona around UCNPs@SiO_2 in normal and cancerous human blood plasma affects the upconversion fluorescence properties of this system.

II. Materials and Methods

Synthesis of up-conversion nanoparticles shelled by SiO_2:

Lanthanide acetate hydrates such as $Y(CH_3CO_2)_3$, $Er(CH_3CO_2)_3$ (99.9%) and $Yb(CH_3CO_2)_3$ (99.9%). 1-Octadecene (90%) and oleic acid (90%) were purchased from Sigma Aldrich. Moreover, NH_4F (96%), NaOH (96%), and solvents, such as methanol, ethanol, acetone, hexane, and cyclohexane, were obtained from Merck Chemical Co. All chemicals were used as-received without further purification.

UCNPs were synthesized using a co-precipitation method [17]. In brief, Yb, Er, Y acetate salts, oleic acid, and 1-octadecene as surfactants were mixed and heated to 150°C under argon. After reaching thermal equilibrium, a methanolic solution of NaOH and NH_4F was added into the flask, after removing methanol by vacuum and heating at 70 °C for 15 min, the mixture was heated up to

300 °C for 10 min and maintained for 1 hour. The resulting nanoparticles were purified by centrifugation, washed with ethanol, and dispersed in hexane for further steps.

To synthesize UCNPs shelled by SiO_2, a mixture of cyclohexane and IGEPAL is sonicated, followed by the addition of nanoparticles and continued sonication, as well as stirring. To the product of the previous step, ammonia is gradually added and left to stir for half an hour. The addition of TEOS is then done dropwise followed by 48 hours of stirring under room temperature and reflux conditions. The product is moved to two tubes and ethanol and acetone are added, sonicated, and centrifuged. The solution is then re-washed with a mixture of ethanol and deionized water. The final product is dispersed and stored in deionized water.

Phosphate-buffered saline (PBS) was prepared by dissolving NaCl, KCl, Na_2HPO_4, and KH_2PO_4 in distilled water at pH 7.4. Normal human blood plasma was obtained from healthy donors who provided informed consent. The blood samples were collected in sterile tubes containing citrate as an anticoagulant and were centrifuged at 3000 rpm for 15 minutes to obtain the plasma.

The morphology, size, and chemical composition of the UCNPs were characterized by transmission electron microscopy (Zeiss EM900 transmission electron microscope). The fluorescence properties were measured by a spectrophotometer.

Sample preparation and analysis techniques:

To investigate the protein corona formation and fluorescence properties of UCNPs shelled by SiO_2 in PBS and normal human blood plasma, the nanoparticles were added to the solutions and incubated at 37°C for different time intervals and the emission was monitored.

The fluorescence properties were measured using the laser diode of 980 nm (MDL-980 from CNI Laser) as a CW excitation light source and a 400 µm core diameter optical fiber guided the light to the sample. A power meter (Ophire Nova II) was used for recording the excitation power; the excitation power density was calculated by the total measured power over the beam profile and the measured beam width. The luminescence emission was measured at an angle of 90° to the excitation path by Avantes spectrometer (Avaspec 2048Tech) collected using a 400 µm core diameter optical fiber (Sma400-Avantes) from the cuvette.

III. RESULTS AND DISCUSSION

The TEM image of UCNPs and nanoparticle size distribution in Fig. 1 shows nanocrystals having an average size of 28.4 nm. As is shown in Fig. 2 according to the dynamic light scattering (DLS) diagram of UCNPs@silica, achieving a shell thickness of approximately 50 nm is evident.

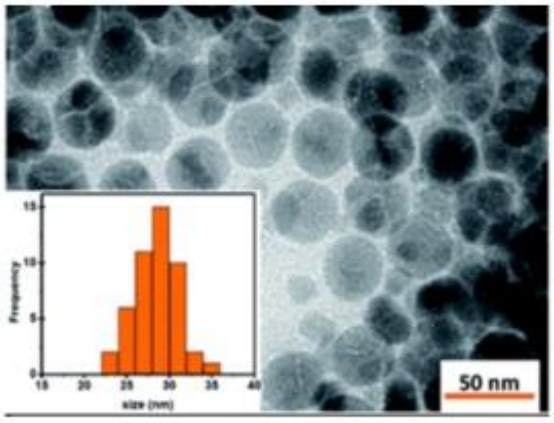

Fig. 1 TEM image and distribution size of UCNPs colloidal suspension.

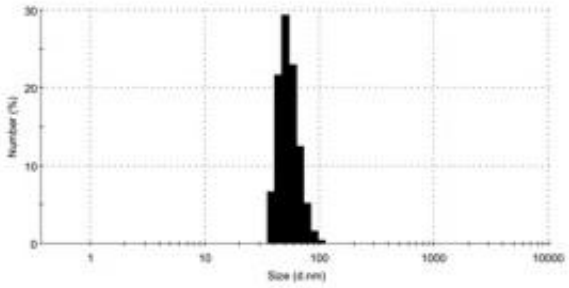

Fig. **2** The distribution size diagram of UCNP@SiO_2 (by DLS)

Figure 3 shows the up-conversion luminescence spectrum and the schematic of

the energy levels of Yb^{3+} as a NIR absorber and Er^{3+} as an activator and allowed energy transitions. The PL spectrum of $NaYF_4$:Yb, Er@$dSiO_2$ has two

main peaks, green and red, which are related to $^4S_{3/2} \rightarrow {}^4I_{15/2}$ and $^4F_{9/2} \rightarrow {}^4I_{15/2}$ transitions.

Table **1** Styles of different parts of the manuscript

emission	wavelength	Radiative transition	anti-Stokes shift
green	544	$^2H_{11/2}$, $^4S_{3/2} \rightarrow {}^4I_{15/2}$	436 nm
red	660	$^4F_{9/2} \rightarrow {}^4I_{15/2}$	320 nm
blue	408	$^2H_{9/2} \rightarrow {}^4I_{15/2}$	572 nm

PL spectra of NaYF4:Yb, Er is a nonlinear process, and also for NaYF4:Yb, Er@dSiO2 PL intensity is dependent on excited power. Figure 3 shows the emission spectrum of up-conversion nanoparticles with a dense silica shell regarding change in the excitation power. The silica-packed layer also does not affect the optical response of nanoparticles. In addition to the hydrophilicity of the surface, the silica-packed layer also protects it. The stability of this structure is also long (three months under review).

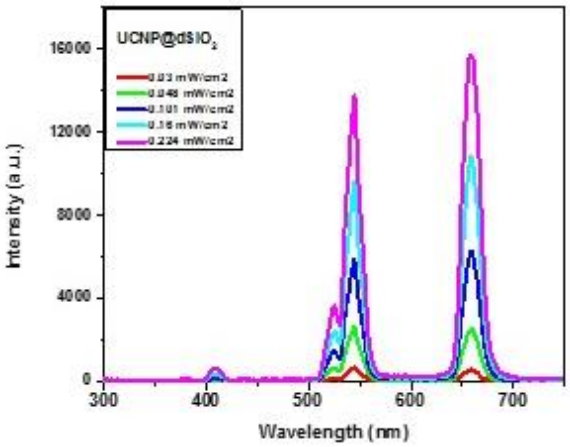

Fig. **3** Upconversion light emission spectrum of UCNP@$dSiO_2$ under 980 nm excitation at different powers.

A very important issue before dealing with any aspect of the application of nanoparticles in the biological environment is that as soon as the nanoparticles enter the biological environment, their surface is surrounded by the proteins of the environment and a unique aura of proteins sits on the surface of the nanoparticles. After intravenous injection, blood is the first biological environment that nanomaterials see. Blood plasma contains more than 3,700 types of proteins. What happens with the presence of nanoparticles in blood plasma is the competition between different molecules to surround the surface of nanoparticles. Worman's effect states that initially, proteins with higher concentrations in the blood adhere to the surface of nanoparticles. Over time, however, other proteins with a greater affinity for absorption replace them. This phenomenon leads to changes in the nanoparticle surface within the biological environment. Consequently, the nanoparticles exhibit new responses, which are dependent on their altered form and are referred to as corona protein. In this study, the emission behavior of synthesized UCNP@SiO_2 in the biological environment and the formed corona are presented as a basis for all future biological studies with these materials. The up-conversion light emission spectrum of UCNP@$dSiO_2$ in healthy human blood plasma in figure 4 shows there is no change in peaks rather than UCNP@$dSiO_2$ in water. this is promising for applications of UCNP@SiO_2.

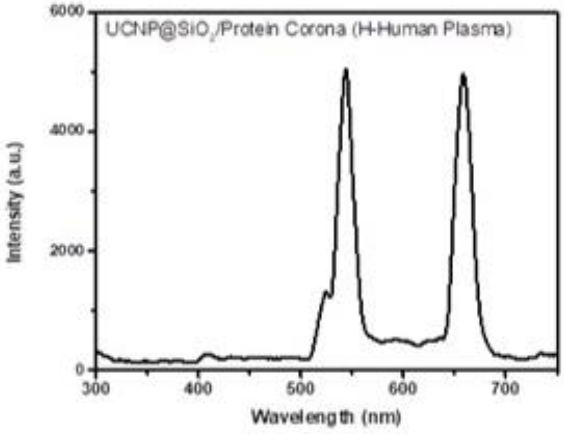

Fig.**4** Up-conversion light emission spectrum of UCNP@$dSiO_2$ in healthy human blood plasma under 980 nm.

In Fig. 5, a comparison of the up-conversion light emission spectrum of UCNP@dSiO$_2$ in BPS, healthy human blood plasma, and cancerous human blood plasma is presented. The peak positions remain constant across all samples, indicating stability. Additionally, since the concentrations of nanoparticles and blood plasma were the same in both healthy and cancerous conditions, it can be inferred that the corona protein formed in the cancerous environment leads to a greater decrease in the release of nanoparticles compared to the healthy environment. This observation highlights the potential utility of this phenomenon as a rapid diagnostic method for cancer.

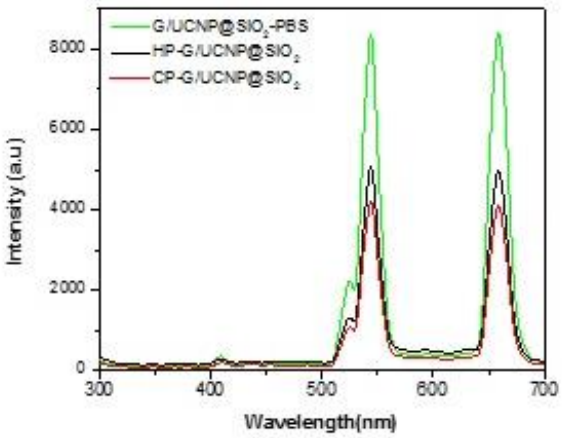

Fig. **5** comparison of upconversion light emission spectrum of UCNP@dSiO$_2$ in BPS, healthy and cancerously human blood plasma under 980 nm.

The formation of a corona on nanoparticles in human blood plasma may be influenced by various factors. While it is commonly assumed that nanoparticles quickly become coated with a layer of proteins and other biomolecules upon introduction into the bloodstream, the results of our study do not definitively support this assumption. Further investigation is needed to clarify the dynamics and factors influencing corona formation on nanoparticles. As time passes, the composition of the protein corona can change due to interactions with other components in the bloodstream. For example, some proteins may dissociate from the nanoparticle surface and be replaced with other proteins, leading to changes in the overall structure and properties of the corona. In addition, understanding the effect of time on the formation of the protein corona is important for developing safe and effective nanoparticles for medical applications. By studying the kinetics of protein corona formation, researchers can gain insights into how to optimize nanoparticle design to minimize immune system recognition and improve their effectiveness as drug delivery vehicles. Corona protein formation is unique for each type of nanoparticle and is formed with its own dynamics.

In the next step, the nanoparticles were injected into the plasma, the spectrum was taken within 5 minutes. The interesting point is that within 100 minutes, each of the peaks did not change appreciably, and this means that the nanoparticles are surrounded by corona protein as soon as they are in the plasma environment, and finally, the formation of hard and soft corona has an effect on the spectrum over time.

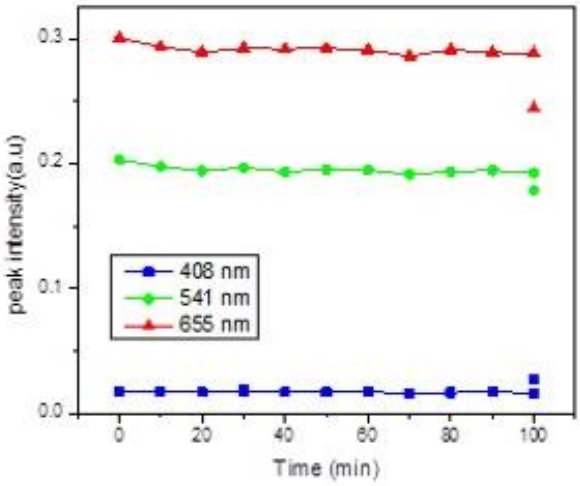

Fig. **6** Peak intensity versus time of corona protein formation.

In Fig. 6, from the moment of injection to 100 minutes later, the intensity changes of each of the 408 nm, 541 nm, and 655 nm peaks can be seen. After 100 minutes, the excess plasma was removed and after centrifugation, the spectrum was taken. The results show a decrease in the intensity of the green and red peaks, which can be partly due to the loss during filtration and the loss of nanoparticles. But the increase of the 408 nm peak is due to the removal of the ambient plasma because it absorbs in this region. Also, the light emission spectrum of

both blue and green emitting nanoparticles was investigated in the presence of healthy and cancerous human plasma. Corona protein of healthy and cancerous samples did not show any special change except for a slight drop. This result indicates that even in the presence of cancer samples, nanoparticles have not lost their light-emitting properties and can be used.

IV. CONCLUSION

Based on other studies, we know that the SiO_2 shells can stabilize UCNPs and prevent their aggregation or decomposition in water. In this work, UCNP@SiO_2 in PBS and normal and cancerous human blood plasma have been studied. Results showed that the fluorescence behavior of UCNPs no changed by the effect of the formation of protein corona in human and cancerous blood plasma and UCNP@SiO_2 can be applicable in biological media for therapy and diagnosis.

REFERENCES

[1] H. Markus, and H. Schäfer, "Upconverting nanoparticles," Angewandte Chemie International Edition, vol. 50, pp. 5808-5829, 2011.

[2] Ch. Bing and F. Wang, "Emerging frontiers of upconversion nanoparticles," Trends in Chemistry, vol. 2, pp. 427-439, 2020.

[3] F. Wang, D. Banerjee, Y. Liu, X. Chen, and X. Liu, "Upconversion nanoparticles in biological labeling, imaging, and therapy," Analyst, vol. 135, pp. 1839-1854, 2010.

[4] Gu. Bin and Q. Zhang. "Recent advances on functionalized upconversion nanoparticles for detection of small molecules and ions in biosystems," Advanced Science, vol. 5, pp. 1700609, 2018.

[5] L. Gungun and D. Jin, "Responsive sensors of upconversion nanoparticles," ACS sensors, vol. 6, pp. 4272-4282, 2021.

[6] G. Kakavelakis, K. Petridis, and E. Kymakis, "Recent advances in plasmonic metal and rare-earth-element upconversion nanoparticle doped perovskite solar cells," Journal of Materials Chemistry A, vol. 5, pp. 21604-21624, 2017.

[7] A. A. Ansari and M. Sillanpää, "Advancement in upconversion nanoparticles based NIR-driven photocatalysts," Renewable and Sustainable Energy Reviews, vol. 151, pp. 111631, 2021.

[8] S. Wen, J. Zhou, K. Zheng, A. Bednarkiewicz, X. Liu, and D. Jin, "Advances in highly doped upconversion nanoparticles," Nature communications, vol. 9, pp. 2415 (1-12), 2018.

[9] D. R. Blanca and D. Jaque, "Upconversion nanoparticles for in vivo applications: limitations and future perspectives," Methods and Applications in Fluorescence, vol. 7, pp. 022001, 2019.

[10] S. Andreas and H. H. Gorris, "Surface modification and characterization of photon-upconverting nanoparticles for bioanalytical applications," Chemical Society Reviews, vol. 44, pp.1526-1560, 2015.

[11] A. A. Ansari, A. K. Parchur, and G. Chen, "Surface modified lanthanide upconversion nanoparticles for drug delivery, cellular uptake mechanism, and current challenges in NIR-driven therapies," Coordination Chemistry Reviews, vol. 457, pp. 214423, 2022.

[12] M. S. Arai and A. SS de Camargo, "Exploring the use of upconversion nanoparticles in chemical and biological sensors: from surface modifications to point-of-care devices," Nanoscale Advances, vol. 3, pp. 5135-5165, 2021.

[13] J.-N. Liu, W.-B. Bu, and J.-L. Shi, "Silica coated upconversion nanoparticles: a versatile platform for the development of efficient theranostics." Accounts of chemical research, vol. 48, pp. 1797-1805, 2015.

[14] D. Drozd, H. Zhang, I. Goryacheva, S. De Saeger, and N. V Beloglazova, "Silanization of quantum dots: challenges and perspectives," Talanta, vol. 205, pp. 120164, 2019.

[15] C. Li, C. Ma, F. Wang, Z. Xi, Z. Wang, Y. Deng, and N. He, "Preparation and biomedical applications of core–shell silica/magnetic nanoparticle composites," Journal of nanoscience and nanotechnology, vol. 12, pp. 2964-2972, 2012.

[16] Ch. Hao, B. Ding, and J. Lin, "Recent progress in upconversion nanomaterials for emerging

optical biological applications," Advanced Drug Delivery Reviews, vol. 188, pp. 114414, 2022.

[17] N. Ghazyani, M. H. Majles Ara, and M. Raoufi, "Nonlinear photoresponse of $NaYF_4$: Yb, Er@ $NaYF_4$ nanocrystals under green CW excitation: a comprehensive study," RSC advances, vol. 10, pp. 25696-25702, 2020.

THIS PAGE IS INTENTIONALLY LEFT BLANK.